

Landmark Sequence Data Association for Simultaneous Localization and Mapping of Robots

Yingmin Yi, Ying Huang

*Faculty of Automation and Information Engineering, Xi'an University of Technology, Xi'an 710048,
Shaanxi, China
Email: yiyim@xaut.edu.cn*

Abstract: *The paper proposes landmark sequence data association for Simultaneous Localization and Mapping (SLAM) for data association problem under conditions of noise uncertainty increase. According to the space geometric information of the environment landmarks, the information correlations between the landmarks are constructed based on the graph theory. By observing the variations of the innovation covariance using the landmarks of the adjacent two steps, the problem is converted to solve the landmark TSP problem and the maximum correlation function of the landmark sequences, thus the data association of the observation landmarks is established. Finally, the experiments prove that our approach ensures the consistency of SLAM under conditions of noise uncertainty increase.*

Keywords: *Landmark sequence, data association, simultaneous localization and mapping, robots.*

1. Introduction

Data association is a key point in simultaneous localization and mapping for robots. The Extended Kalman Filter formulation of Simultaneous Localization And Mapping (EKF-SLAM) is fundamental for solving SLAM problem. References

[6, 7] present the consistency estimate of EKF-SLA and FastSLAM. The researches indicate that the data association approach directly affects the accuracy of the consistency estimate. Data association defines the process of sensor establishing the correlations between its measurements and the targets. Paper [6] shows that data association is crucial to solve SLAM problem. Incorrect data association may result in infinity of SLAM, even the failure of the whole SLAM process.

There are already certain achievements in the studies of data association algorithms – mainly including three categories: first, the Nearest Neighbor (NN) data association; second, Joint Probabilistic Data Association (JPDA) for multiple targets; third, correlation data association based on graph theory. In [10] the authors propose the nearest neighbour data association, which is easy in implementation, but worse in interferences resistance. The probability data association is applicable only for a single target scenario. In JPDA for multiple targets it is difficult in obtain the probabilities of the joint events and the correlated events and it will be subjected to combination exploration due to the echo density increase. So the scholar of this paper proposes a compromising approximation algorithm. Paper [11] proposes the Takagi-Sugeno Data Association (TSDA), compared to JPDA, the computation complexity is reduced.

In [12] 3SCAN-JPDA algorithm is proposed, which is applied in real time dynamic environment, reducing the computations. For clutter environment, [8] proposes the Joint Compatibility Branch and Bound (JCBB). For higher correlation accuracy [13] multi-target correlation algorithm is suggested – Ant Colony-Genetic Algorithm Data Association (AC-GADA). By using the information of the characteristics of the landmarks, the layout of the landmark groups and the deviation bounds between the landmark prediction and the observation, references [14-16] propose an improved probabilistic data association algorithm. In [17, 18] the Maximum Common Subgraph (MCS) is proposed which is based on the graph theory. But it is difficult to solve the NP issue in searching for the maximum common subgraph of the two complete graphs. The MCS approach and the JCBB approach both utilize the available correlation information for batch correlations. Via the pre-set hypothesis and by explaining the hypothesis on the search tree, JCBB takes the hypothesis, corresponding to the best explanation as the reliable data association. MCS is divided into two steps: first, compiling to constraints; second, conducting the search for the maximum compatible constraint. Under conditions of noise uncertainty increase, due to the independence between the observed information and landmarks, the matching will fail or the estimation error will increase.

2. Landmark sequence data association

Simultaneous localization and mapping for robots are based on data association. For the situation of noise uncertainty increase, this paper inducts the TSP problem in the SLAM problem. By calculating the maximum correlation function of the TSP sequences, the landmark sequence data association can be obtained and the map can be updated.

2.1. The classic EKF-SLAM approach

The simultaneous localization and mapping for EKF-based robots is based on the minimum mean squared error, realizing the optimum recursive process for the robot poses in the time domain. This approach is divided into two steps, namely prediction and updating. First, send the control signals and the odometer information to the state equation of the robot system and complete the predictions of the poses and map landmarks. Second, by the observation and extraction of the environment landmarks, update the robot poses and the landmark map.

The predictions are:

$$(1) \quad \hat{\mathbf{x}}_{k|k-1} = f(\hat{\mathbf{x}}_{k-1|k-1}, \mathbf{u}_k),$$

$$(2) \quad \mathbf{P}_{xx,k|k-1} = \nabla f \mathbf{P}_{xx,k-1|k-1} \nabla f^T + \mathbf{Q}_k,$$

where $\hat{\mathbf{x}}_{k|k-1}$ represents the estimate of the pose state vector of the robot during the state shifting from time $k-1$ to k ; \mathbf{u}_k represents the control vector during the state shifting from time $k-1$ to k ; $f(\cdot)$ represents the odometer model; \mathbf{Q}_k represents the system white noise covariance; ∇f is the Jacobian matrix of f regarding the estimates $\hat{\mathbf{x}}_{k-1|k-1}$; $\mathbf{P}_{xx,k|k-1}$ is the pose covariance matrix during the state shifting from time $k-1$ to k , denoted as $\mathbf{P}_{k|k-1}$ for short [21].

Then the updates are:

$$(3) \quad \begin{bmatrix} \hat{\mathbf{x}}_{k|k} \\ \hat{\mathbf{m}}_k \end{bmatrix} = \begin{bmatrix} \hat{\mathbf{x}}_{k|k-1} \\ \hat{\mathbf{m}}_{k-1} \end{bmatrix} + \mathbf{W}_k [\mathbf{z}(k) - h(\hat{\mathbf{x}}_{k|k-1}, \hat{\mathbf{m}}_{k-1})],$$

$$(4) \quad \mathbf{P}_{k|k} = \mathbf{P}_{k|k-1} - \mathbf{W}_k \mathbf{S}_k \mathbf{W}_k^T.$$

Here

$$(5) \quad \mathbf{S}_k = \nabla h \mathbf{P}_{k|k-1} \nabla h^T + \mathbf{R}_k,$$

$$(6) \quad \mathbf{W}_k = \mathbf{P}_{k|k-1} \nabla h^T \mathbf{S}_k^{-1},$$

and $\hat{\mathbf{m}}_k$ represents the estimate of the landmark vector of the static location i at time k ; \mathbf{z}_{ik} represents the observed location by the robot from landmark i at time k , denoted as $\mathbf{z}(k)$ for short; $h(\cdot)$ represents the heading observation model; \mathbf{R}_k is the observation white noise covariance; ∇h is the Jacobian matrix of h regarding the estimates $\hat{\mathbf{x}}_{k|k-1}$ and $\hat{\mathbf{m}}_{k-1}$.

2.2. The landmark TSP problem based on the simulated annealing algorithm

The landmarks of the SLAM problem for robots are comparable to the cities of TSP problem. The coordinate of the landmark represents the location of the city and the distance between the cities can be calculated by their coordinates. In SLAM problem, we always suppose that the landmarks are stationary. Hence, the optimum solution of the landmark TSP problem is unique. Due to the observation noise, all the landmarks within the observation area are regarded as known conditions in TSP

problem. The simulated annealing algorithm is suitable for dealing with global optimization and discrete variable optimization problems. The simulated annealing algorithm of the landmark TSP problem is shown in Fig. 1.

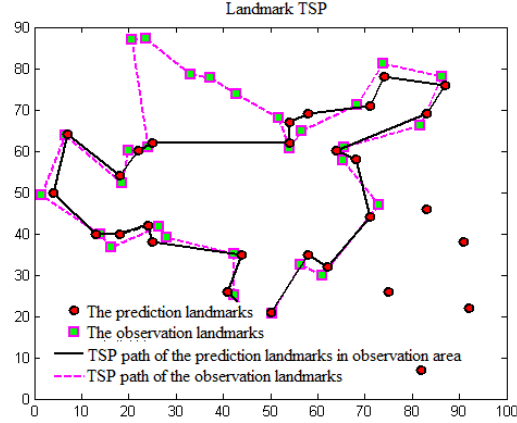


Fig. 1. The landmark TSP problem based on the simulated annealing algorithm

By calculating the TSP problem for the prediction landmarks (prediction for the observed landmarks in the observation area), the optimum TSP path can be obtained. Besides, the optimum TSP path can be also obtained by calculating the TSP problem of the observation landmarks).

2.3. The correlation functions of the landmark sequence

Regarding the coordinates of the landmarks as independent variables, the landmarks are two-dimensional discrete points. According to the TSP path, a permutation of a set of landmarks can be obtained. Every permutation is a landmark sequence, namely the lines between the landmarks represent a fixed time period. The sequences are signals. According to the two landmark sequences corresponding to the maximum correlation function, the correlations of the common landmarks can be ensured.

2.4. The landmark sequence data association

The main process of the landmark sequence data association is as follows. First, calculate the TSP problem of the prediction landmarks and the observation landmarks to obtain the TSP sequences; second, calculate the maximum correlation function of the two sequences and mark the observed landmarks and the new observed landmarks; at last, correlate the landmarks and update the map.

The specific steps are six.

Step 1. Initialization and data association

$$(7) \quad \begin{aligned} \hat{\mathbf{x}}_{k|k-1} &= \mathbf{F}_{k-1} \mathbf{x}_{k-1}, \\ \mathbf{P}_{k|k-1} &= \mathbf{F}_{k-1} \mathbf{P}_{k-1|k-1} (\mathbf{F}_{k-1})^T + \mathbf{Q}_{k-1}. \end{aligned}$$

Predict the observed landmarks. The observed landmarks remaining in the current observation area are denoted as prediction landmarks.

Conduct prediction for the landmarks to get the observation landmarks. Regard the landmarks as cities in TSP problem. Use the coordinates of the landmarks to denote the locations of the cities and calculate the distances between the cities.

Step 2. Solve the landmark TSP problem

Solve the TSP problem for the prediction landmarks and the observation landmarks to get the landmark permutation. Regard the landmark permutation as a two-dimensional sequence respecting to the coordinates and obtain two sets of sequences

Step 3. Calculate the correlation functions of the sequences

Calculate the correlation functions of the two sequences. Obtain the sequence length via the prediction landmark combination. Divide the observation landmark combination sequences into observed landmarks \mathbf{z}_{k0} and new observed landmarks

$\mathbf{z}_{k,k-1}$:

$$(8) \quad \mathbf{z}_k = \begin{bmatrix} \mathbf{z}_{k0} \\ \mathbf{z}_{k,k-1} \\ \mathbf{z}_{nk} \end{bmatrix}.$$

Step 4. Solve the TSP problem for the observed landmarks

Solve the TSP problem for the observed landmarks to obtain the observed landmark sequence permutation.

Step 5. Calculate the observed landmark sequence

Calculate the correlation functions for the observed landmark sequence permutation and the prediction landmark sequence and choose the observed landmark sequence corresponding to the maximum correlation function.

Step 6. Map correlation

Conduct the landmark correlations for map building on the observed landmark sequence and the prediction landmark sequence. Then add the new observed landmarks to the map.

$$(9) \quad \begin{aligned} \mathbf{x}_k^{\text{new}} &= h^{-1}(\mathbf{z}_{nk}, \mathbf{x}_{vk}), \\ \mathbf{x}_k &= \begin{bmatrix} \mathbf{x}_k & \mathbf{x}_k^{\text{new}} \end{bmatrix}^T. \end{aligned}$$

To validate the consistency estimate of the algorithm, a Normalized Estimation Error Squared (NEES) is used to evaluate the performances of the filtering estimate, under linear Gaussian filter [20].

$$(10) \quad \varepsilon_k = (\mathbf{x}_k - \hat{\mathbf{x}}_{k|k})^T \mathbf{P}_{k|k}^{-1} (\mathbf{x}_k - \hat{\mathbf{x}}_{k|k}).$$

Namely, for filtering the estimate of the approximate Gaussian distribution, NEES follows χ^2 distribution. The measure of filter consistency is found by examination of the average NEES over N Monte Carlo runs of the filter; $\bar{\varepsilon}_k$ approaches to the dimensions of the state-vector when $N \rightarrow \infty$:

$$(11) \quad \bar{\varepsilon}_k = \frac{1}{N} \sum_{i=1}^N \varepsilon_{ik}.$$

Namely, for Gaussian filter, $\bar{\varepsilon}_k$ is a density function following χ^2 distribution with N degrees of freedom. The pose space of the robot is a three-dimensional vector. The probability over 50 Monte Carlo runs is 95%, with confidence interval of [2.36, 3.72]. It is optimistic when it is greater than 3.72 and conservative when it is less than 2.36.

3. Experiments and analysis

The advancement of networking and multimedia technologies enable the distribution and sharing of multimedia content widely. Fig. 2 shows the experiment platform of MT-R robots. The MT-R robot is two-wheel driven, equipped with a PTZ camera of two-degrees of freedom, an ultrasound sensor, a speed measuring coder and other sensors.

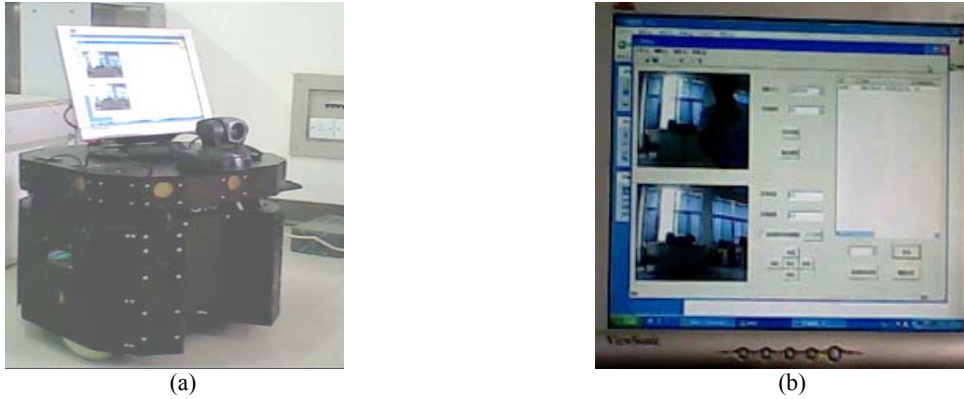


Fig. 2. The experimental verification platform: the mobile robot experimental test platform (a); the developed experimental test system (b)

The experiments compared the typical data association approaches. NN, JCBB and LSDA are all carried out for SLAM of robots. The first group of experiments is under low noise environment. The initial condition is $P_0 = \text{diag}[1 \times 10^{-4}, 1 \times 10^{-4}, 1 \times 10^{-4}]$, $Q_0 = \text{diag}[0.3^2, (3.0 * p_i / 180)^2]$, and $R = \text{diag}[0.1^2, (1.0 * p_i / 180)^2]$. The second group of experiments is under high noise environment. The initial condition is $P_0 = 10 * \text{diag}[1 \times 10^{-4}, 1 \times 10^{-4}, 1 \times 10^{-4}]$ and $Q_0 = 10 * \text{diag}[0.3^2, (3.0 * p_i / 180)^2]$, $R = 10 * \text{diag}[0.1^2, (1.0 * p_i / 180)^2]$.

The experiments are about the SLAM data of the data association approaches under conditions of noise uncertainty increase Fig. 3, where * denotes the landmark on the map; + denotes the prediction location with respect to the landmark. The ellipse denotes the prediction location area regarding the landmark. The segment

denotes the lines between the headings. The curve denotes the practical path of the robot. Fig. 3a is the partial magnified SLAM-graph under NN data association. Fig. 4a is the SLAM-graph under JCBB data association. Fig. 4b is the partial magnified SLAM-graph under JCBB data association. Fig. 5a is the SLAM-graph under LSDA data association. Fig. 5b is the partial magnified SLAM-graph under LSDA data association.

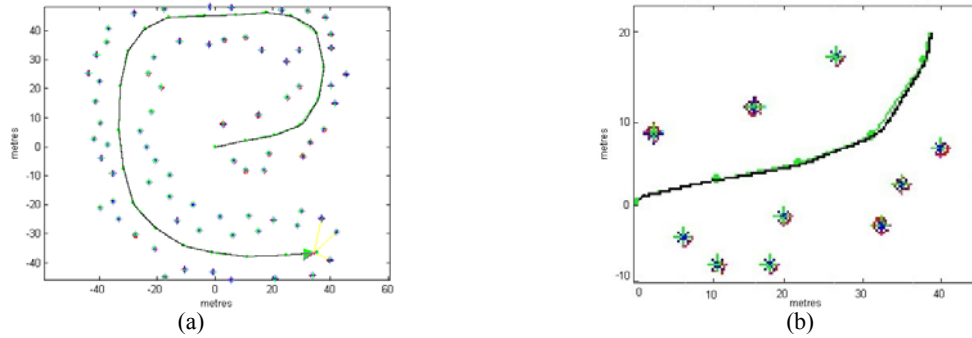


Fig. 3. The SLAM test based on NN data association in the case of uncertainty noise increasing: the SLAM test based on NN data association (a); the partial SLAM map based on NN data association (b)

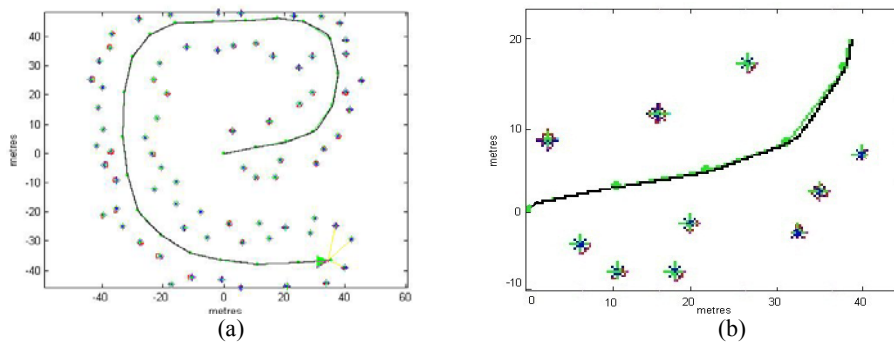


Fig. 4. The SLAM test based on JCBB data association in the case of uncertainty noise increasing: the SLAM test based on JCBB data association (a); the partial SLAM map based on JCBB data association (b)

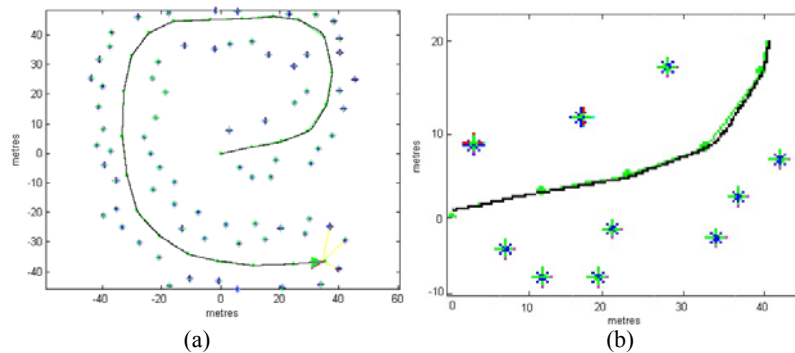


Fig. 5. The SLAM test based on LSDA data association in the case of uncertainty noise increasing: the SLAM test based on LSDA data association (a); the partial SLAM map based on LSDA data association (b)

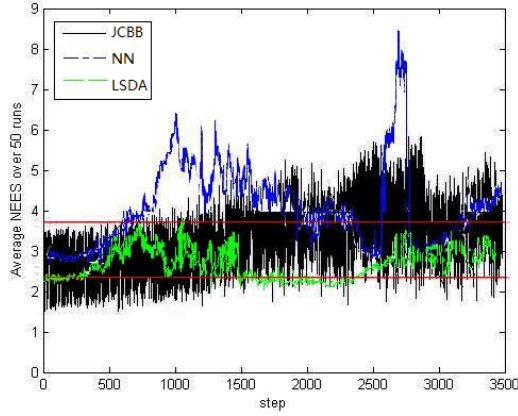


Fig. 6. The estimation consistency by data association methods in the case of low uncertainty noise

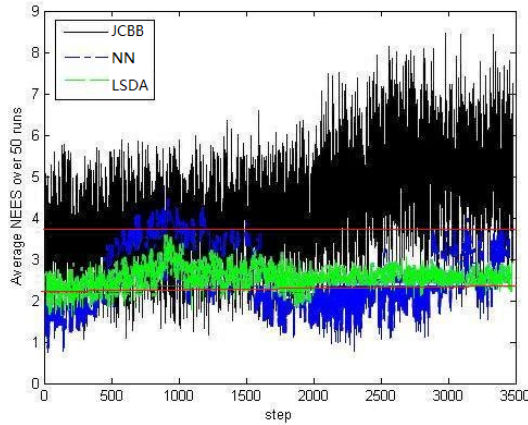


Fig. 7. The estimation consistency by data association methods in the case of uncertainty noise increasing

By comparing the results of Fig. 5 with Figs 3 and 4, we can see that in the map built with NN approach and JCBB approach, there are deviations between the estimates and the practical landmarks; however, in the map built with LSDA approach, the estimates almost coincide with the practical landmarks.

To validate the consistency estimate of the proposed approach, we have conducted 50 experiments for the three approaches to compare the pose consistency estimates under different noise conditions. Fig. 6 shows the NEES data of the experiments of the three approaches in a low noise environment.

As it can be seen from Fig. 6, in a low noise environment, the NEES curves under NN and JCBB approaches are mostly out of the confidence interval, which is regarded as conservative. Meanwhile, the NEES curves under LSDA approach are mostly within the confidence interval, which is regarded as optimistic.

Fig. 7 shows the NEES data of the experiments of the three approaches in a high noise environment.

As it can be seen from Fig. 7, in a high noise environment, the NEES curves under NN and JCBB approaches have vigorous vibrations partially, most of which

are out of the confidence interval, regarded as conservative; the NEES curves under LSDA approach are mostly within the confidence interval, regarded as optimistic.

From the experiments above, the proposed approach keeps an optimistic consistency estimate for SLAM under conditions of noise uncertainty increase. The approach is superior to the NN data association and JCBB association in general.

4. Conclusion

This paper proposes the landmark sequence data association for SLAM of robots, which is against the condition of system noise uncertainty increase. By using the comparable city TSP problem, first the correlation functions of the landmarks are calculated out. Then the data associations between the observation landmarks and the prediction landmarks are established. Finally, the map is updated. The experiments validate that the landmark sequence data association keeps the consistency estimate of the algorithm optimistic under conditions of noise uncertainty increase.

Acknowledgements: This work was supported by the National Natural Science Foundation of China (No 51275405) and the science research programs of the Education department of Shaanxi Province (2013JK1078).

References

1. Uyen, H. S. V., J. W. Jeon. Combine Kalman Filter and Particle Filter to Improve Color Tracking Algorithm. – In: Proc. of International Conference on Control, Automation and Systems 2007, 558-561.
2. Anati, R., D. Scaramuzza, K. G. Derpanis, K. Daniilidis. Robot Localization Using Soft Object Detection. – In: Proc. of IEEE International Conference on Robotics and Automation (ICRA'2012), 2012, 4992-4999.
3. Ivanjko, E., M. Uasak, I. Petrovic. Kalman Filter Theory Based Mobile Robot Pose Tracking Using Occupancy Grid Maps. – In: Proc. of International Conference on Control and Automation (ICCA'2005), 2005, 869-874.
4. Smith, R., P. M. Cheeseman. Estimating Uncertain Spatial Relationships in Robotics. – *Uncertainty in Artificial Intelligence*, 1988, 435-461.
5. Smith, R., M. Self, P. Cheeseman. A Stochastic Map for Uncertain Spatial Relationships. – In: Proc. of IEEE: International Symposium of Robotics Research, 1987, 467-474.
6. Bailey, T., J. Nieto, J. Guivant, et al. Consistency of the EKF-SLAM Algorithm. – In: Proc. of IEEE/RSJ Int. Conf. on Intelligent Robots and Systems. Beijing: IEEE, 2006, 3562-3568.
7. Bailey, T., J. Nieto, E. Nebot. Consistency of the Fast SLAM Algorithm. – In: Proc. of IEEE Int. Conf. on Robotics and Automation. Orlando: IEEE, 2006, 424-429.
8. Neira, J., J. D. Tardos. Data Association in Stochastic Mapping Using the Joint Compatibility Test. – *IEEE Transactions on Robotics and Automation*, Vol. **17**, 2001, No 6, 890-897.
9. Yi, Yingmin, Ding Liu. Color-State-Noise Simultaneous Localisation and Mapping for Wheel Robots. – *Chinese Journal of Electronics*, Vol. **38**, 2010, No 6, 1339-1243.
10. Singer, R. A., R. G. Sea. A New Filter for Optimal Tracking in Dense Multitarget Environments. – In: Proc. of 9th Allerton Conference Circuit and System Theory, Urbana-Champaign, USA, 1971, 201-211.

11. Watanabe, K., C. D. Pathirana, K. Izumi. T-S Fuzzy Model Adopted SLAM Algorithm with Linear Programming Based Data Association for Mobile Robots. – In: Proc. of IEEE International Symposium on Industrial Electronics (ISIE'2009), 2009, 244-249.
12. Wong, R. H., Xiao Jizhong, S. L. Joseph. A Robust Data Association for Simultaneous Localization and Mapping in Dynamic Environments. – In: Proc. of IEEE International Conference on Information and Automation (ICIA'2010), 2010, 470-475.
13. Shu, Yuan, Yuan Donghui, Sun Jizhou, Liu Yongbo, Li Jing, Yuan Lin. The Application of AC-GA on Multi-Sensor Multi-Target Tracking. – Chinese Journal of Electronics, Vol. **41**, 2013, No 3, 609-614.
14. Maksarov, D. H. Durrant-Whyte. Mobile Vehicle Navigation in Unknown Environments: A Multiple Hypothesis Approach. – IEEE Proc. Control Theory Application, Vol. **142**, 1995, No 4, 385-391.
15. Guivant, J., E. Nebot. Optimization of the Simultaneous Localization and Map-Building Algorithm for Real-Time Implementation. – IEEE Transactions on Robotics and Automation, Vol. **17**, 2003, No 3, 242-257.
16. Castellanos, J. A., J. M. M. Montiel, J. Neira, et al. The SPmap: A Probabilistic Framework for Simultaneous Localization and Map Building. – IEEE Transactions on Robotics and Automation, Vol. **15**, 1999, No 5, 948-952.
17. Bailey, T., E. Nebot. Localisation in Large-Scale Environments. – Robotics and Autonomous Systems, Vol. **37**, 2001, No 4, 261-281.
18. Bailey, T., E. M. Nebot, J. K. Rosenblatt, H. F. Durrant-Whyte. Data Association for Mobile Robot Navigation: A Graph Theoretic Approach. – In: Proc. of IEEE International Conference on Robotics and Automation, 2000, 2512-2517.
19. Jeong, C. S., M. H. Kim. Fast Parallel Simulated Annealing for Traveling Salesman Problem. – In: Proc. of International Joint Conference (IJCNN'1990), San Diego, CA, 1990, 947-953.
20. Bar-Shalom, Y., X. R. Li, T. Kirubarajan. Estimation with Applications to Tracking and Navigation. Toronto, John Wiley and Sons, 2001, 234-235.
21. Krajić, V., N. Stojković. Improvement of Robot Trajectory Tracking by Using Nonlinear Control Methods. – Engineering Review, Vol. **26**, 2006, No 1, 7-17.